

Competitive Antagonism of Glutamate Receptor Channels by Substituted Benzazepines in Cultured Cortical Neurons

KENTON J. SWARTZ, WALTER J. KOROSHETZ, ALUN H. REES, and JAMES E. HUETTNER¹

Department of Neurobiology, Harvard Medical School, Boston, Massachusetts 02115 (K.J.S., J.E.H.), Department of Neurology, Massachusetts General Hospital, Boston, Massachusetts 02114 (W.J.K.), Department of Chemistry, Trent University, Peterborough, Ontario, K9J 7B8 Canada (A.H.R.), and Department of Cell Biology and Physiology, Washington University Medical School, St. Louis, Missouri 63110 (J.E.H.)

Received February 25, 1992; Accepted March 25, 1992

SUMMARY

Whole-cell recordings from rat cortical neurons in dissociated cell culture were used to study the antagonism of glutamate receptors by several lipophilic benzazepine analogues of 2,5-dihydro-2,5-dioxo-3-hydroxy-1*H*-benzazepine (DDHB). DDHB and three substituted derivatives, 4-bromo-, 7-methyl-, and 8-methyl-DDHB, inhibited the activation of *N*-methyl-D-aspartate (NMDA) receptors at both the NMDA recognition site and the glycine allosteric site. In addition, all four compounds blocked the activation of non-NMDA receptors by kainate and L-glutamate. Antagonism by the four benzazepines was equivalent at holding potentials from -80 mV to +50 mV. Both the onset of and recovery from block of the agonist-gated currents were complete within seconds. Antagonist affinity was calculated from the displacement of steady state concentration-response curves for kainate, L-glutamate, glycine, and NMDA, based on the Gaddum-Schild relationship (dose ratio = $1 + [\text{antagonist}]/K_B$). The most potent blocker, 8-Me-DDHB, had an apparent disso-

ciation constant (K_B) of 470 nM at the glycine allosteric site and 27 μM at the NMDA recognition site. The apparent dissociation constant of 8-Me-DDHB for non-NMDA receptors was 6.4 μM when kainate was the agonist and 9.6 μM when L-glutamate was the agonist. Unsubstituted DDHB showed slightly higher affinity for the NMDA recognition site ($K_B = 16 \mu\text{M}$) but was less potent than 8-Me-DDHB at the glycine allosteric site and at non-NMDA receptors ($K_B = 3$ and 65 μM , respectively). At all three sites, the inhibitory actions of these benzazepine derivatives were consistent with a simple competitive mechanism of antagonism. In addition, the antagonist potency of the parent compound, DDHB, against kainate, NMDA, and glycine was equal to or greater than that of other bicyclic antagonists, including kynurenic acid, indole-2-carboxylic acid, and quinoxaline-2,3-dione. Substituted benzazepines represent a new class of glutamate receptor antagonists that show competitive action, significant potency at multiple sites, and a high degree of lipophilicity.

The amino acid L-glutamate activates a number of receptors on the surface of vertebrate central neurons, including two receptor subtypes that are directly coupled to ion channels (1, 2). NMDA is a selective agonist for one of these receptors, which controls the gating of ion channels permeable to Na^+ , K^+ , and Ca^{2+} (3, 4). Physiological concentrations of extracellular Mg^{2+} block NMDA receptor-gated channels, in a voltage-dependent manner (3-6). In addition to the transmitter binding site recognized by NMDA and L-glutamate, the NMDA receptor also possesses an allosteric modulatory site that can be activated by glycine and D-serine (7-9). Recent work (8, 10) suggests that occupation of the glycine site is absolutely required for channels to be opened by NMDA.

This work was supported by a Mahoney Institute Fellowship (K.J.S.), by National Institutes of Health Grants NS 10828 (W.J.K.) and NS 02253 (Bruce P. Bean, Principal Investigator), and by the Klingenstein Foundation (J.E.H.).

¹ Present address: Department of Cell Biology and Physiology, Washington University Medical School, 660 South Euclid Avenue, Box 8228, St. Louis, MO 63110.

The second major class of glutamate receptor that is coupled to an ion channel is the non-NMDA or kainate/AMPA receptor. In central neurons, non-NMDA receptors exhibit rapid desensitization to the agonists L-glutamate, quisqualate, and AMPA but little or no desensitization to kainate and domoate (11). The currents activated by these agonists display linear current-voltage relations and are carried predominantly by monovalent cations (4, 5). In some cell populations, however, kainate elicits an inwardly rectifying current that is largely carried by Ca^{2+} (12). In addition, rat dorsal root ganglion cells express a form of non-NMDA receptor that exhibits desensitization to all kainate/AMPA receptor agonists (13). The recent expression of cloned subunits of the non-NMDA receptor has begun to provide a molecular explanation for the heterogeneity observed in responses to non-NMDA agonists (14, 15). In addition to NMDA and non-NMDA receptors, L-glutamate can also activate several types of "metabotropic receptor" that are linked to GTP-binding proteins (reviewed in Ref. 16).

ABBREVIATIONS: NMDA, *N*-methyl-D-aspartate; AMPA, α -amino-3-hydroxy-4-methylisoxazolepropionic acid; DDHB, 2,5-dihydro-2,5-dioxo-1*H*-benzazepine; DDHB, 2,5-dihydro-2,5-dioxo-3-hydroxy-1*H*-benzazepine; 4-Br-DDHB, 7-Me-DDHB, and 8-Me-DDHB, 4-bromo-, 7-methyl-, and 8-methyl-derivatives of DDHB, respectively; CNS, central nervous system; HEPES, 4-(2-hydroxyethyl)-1-piperazineethanesulfonic acid; EGTA, ethylene glycol bis (β -aminoethyl ether)-*N,N,N',N'*-tetracetic acid.

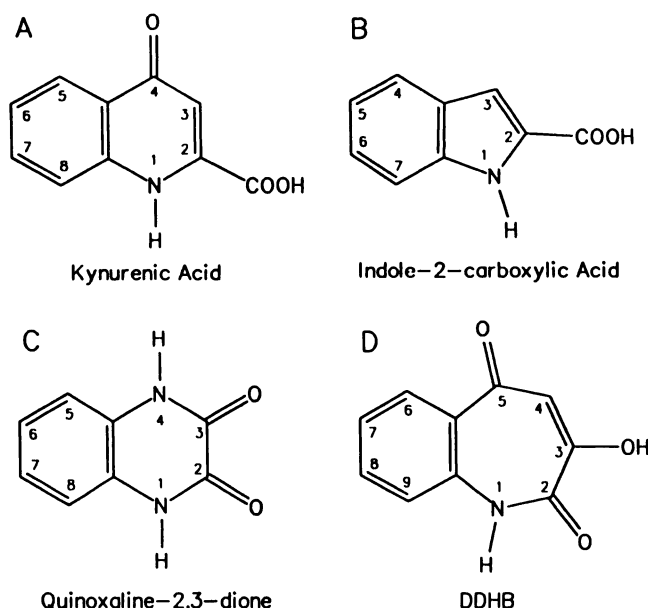


Fig. 1. Parent structures of glutamate receptor antagonists.

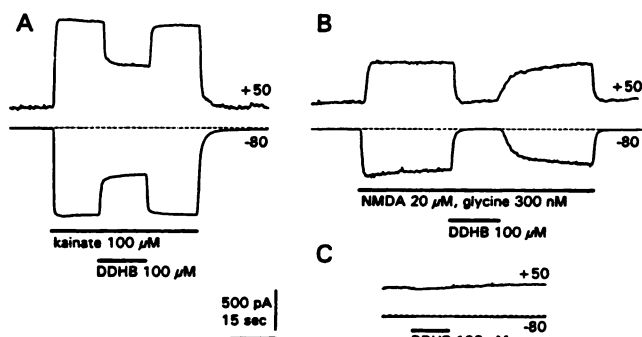


Fig. 2. Antagonism by DDHB is independent of membrane potential. Inhibition produced by 100 μ M DDHB of currents evoked by 100 μ M kainate (A) or 20 μ M NMDA plus 300 nM glycine (B), at holding potentials of +50 mV and -80 mV. With these concentrations, DDHB completely blocked the response to NMDA plus glycine at both holding potentials. Inhibition of current evoked by kainate was to $59 \pm 3.6\%$ of control at -80 mV (five experiments) and to $55 \pm 1.5\%$ of control at +50 mV (three experiments). This difference is not significant at $p < 0.05$ (Student's t test). C, Application of 100 μ M DDHB alone had no effect at +50 or -80 mV.

Non-NMDA receptors underlie the rapid depolarization of postsynaptic neurons at excitatory synapses, whereas NMDA receptors prolong the falling phase of the excitatory postsynaptic potential. Calcium that enters through the channels gated by the NMDA receptor is thought to regulate the long term strength and stability of synaptic connections (17). In addition to their physiological role in excitatory synaptic transmission, both NMDA and non-NMDA receptors have been shown to contribute to excitotoxic neuronal death (18). These neurotoxic actions of L-glutamate, and possibly other endogenous excitatory amino acids, have been implicated in a number of neurological diseases, including ischemia, epilepsy, and Huntington's disease (18, 19). Although the precise mechanisms by which L-glutamate and its analogues destroy neurons have not yet been fully explained, considerable evidence (19) suggests that antagonists of NMDA and non-NMDA receptors may prevent neuronal degeneration in these pathological states.

Kynurenic acid (Fig. 1A) was one of the first compounds reported to block the excitatory actions of L-glutamate on CNS

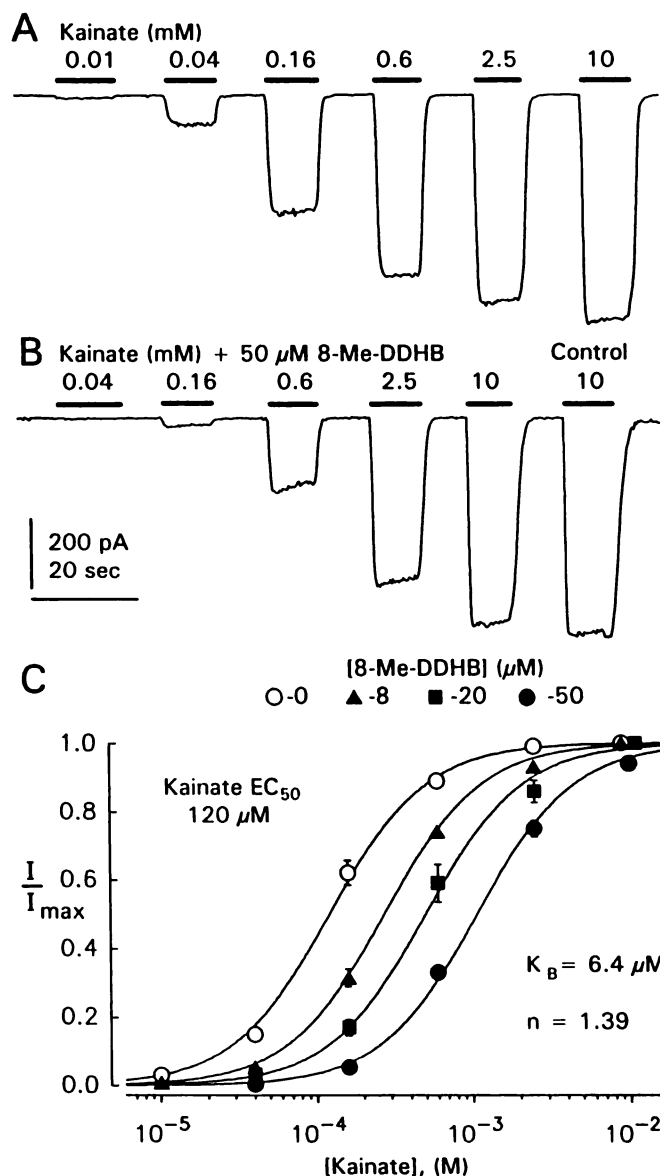


Fig. 3. Competitive antagonism of kainate currents by 8-Me-DDHB. A, Currents activated by 10 μ M to 10 mM kainate. B, In a different cell, currents elicited by 40 μ M to 10 mM kainate with 50 μ M 8-Me-DDHB and a control response to 10 mM kainate alone. Holding potential, -70 mV. C, Concentration-response relations for kainate alone (○) (13 applications in four cells) or in the presence of 8 μ M 8-Me-DDHB (▲) (13 applications in five cells), 20 μ M 8-Me-DDHB (■) (eight applications in five cells), or 50 μ M 8-Me-DDHB (●) (seven applications in three cells). Points, mean \pm standard error of the normalized currents (I/I_{max}). Smooth curves, best fit of eq. 2 to all of the data points for all four antagonist concentrations (0, 8, 20, and 50 μ M), with agonist $EC_{50} = 120 \mu$ M (111–131 μ M, 95% confidence interval), slope factor = 1.39 (1.29–1.47), and antagonist $K_B = 6.4 \mu$ M (5.5–7.5 μ M). Individual fits of eq. 1 were not significantly better, at the 5% level, than the simultaneous fit achieved with eq. 2 ($F_{5,197} = 0.71$).

neurons (20). Further work (21–24) has shown kynurenic acid to be a broad spectrum antagonist, with highest potency at the glycine potentiation site and much lower affinity for the NMDA and non-NMDA recognition sites. Several derivatives of kynurenic acid, as well as a number of related aromatic compounds, have been discovered that exhibit considerably higher affinity for one or more of these sites. Addition of chlorine to the 7-position (22) or to both the 5- and 7-positions (25, 26) of kynurenic acid was found to enhance greatly the affinity for

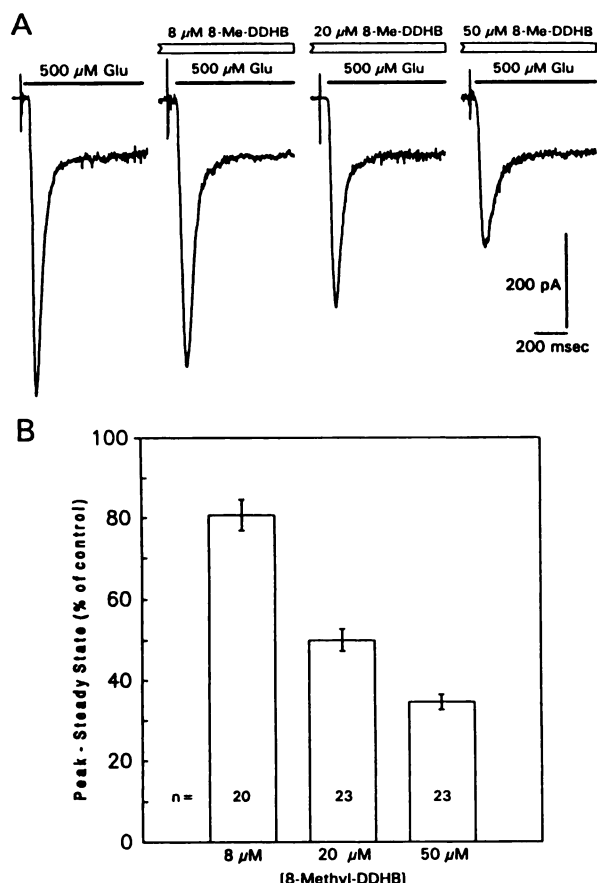


Fig. 4. Inhibition by 8-Me-DDHB of the initial transient current activated by L-glutamate (Glu). **A**, Currents activated by rapid application of 500 μ M L-glutamate alone or with 8, 20, or 50 μ M 8-Me-DDHB. For each application of L-glutamate that included 8-Me-DDHB, the cell was first equilibrated in control external solution containing 8-Me-DDHB at the same concentration. Dizocilpine (MK-801) was included in all solutions, at 1 μ M, to block NMDA receptor channels. Holding potential, -70 mV. **B**, Peak inward current minus steady state current, expressed as a percentage of the control response (peak current minus steady state current for 100 μ M L-glutamate alone). Bars, mean \pm standard error for 8 μ M (20 applications in eight cells), 20 μ M (23 applications in nine cells), and 50 μ M (23 applications in 10 cells) 8-Me-DDHB.

the glycine allosteric site. Contraction of the nitrogen heterocycle to form indole-2-carboxylic acid (10) (Fig. 1B) also yields compounds with relatively high selectivity for the glycine site, compared with the NMDA and non-NMDA agonist recognition sites. Quinoxaline-2,3-diones (Fig. 1C), which lack the 2-carboxyl group, generally show higher affinity for non-NMDA receptors, moderate potency against the glycine allosteric site, and relatively weak activity at the NMDA recognition site (27–31). In the present study, we report the characterization of a series of benzazepines in which the nitrogen-containing heterocycle has been expanded to seven members (32, 33) (Fig. 1D). These compounds represent a new class of competitive glutamate receptor antagonists with high affinity for the glycine allosteric site and modest potency at the binding sites for NMDA and non-NMDA agonists.

Materials and Methods

Compounds. L-Glutamate, glycine, kainate, NMDA, and D-serine were obtained from Sigma, whereas (+)-quisqualate was purchased from Research Biochemicals Inc. The benzazepines DDHB, 8-Me-

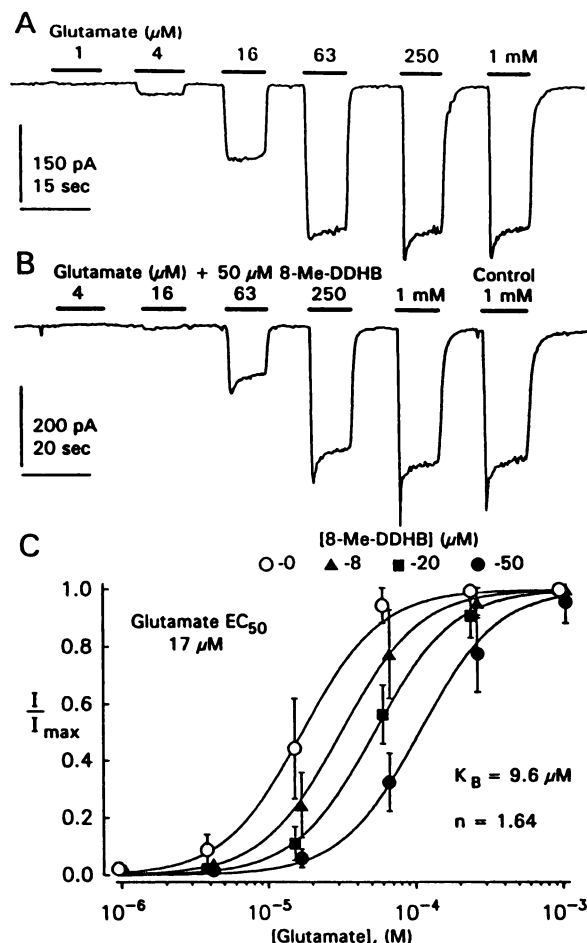


Fig. 5. Competitive antagonism by 8-Me-DDHB of steady state current activated by L-glutamate. **A**, Currents activated by 1 μ M to 1 mM L-glutamate. **B**, In a different cell, currents evoked by 4 μ M to 1 mM L-glutamate with 50 μ M 8-Me-DDHB and a control response to 1 mM glutamate alone. Holding potential, -70 mV. Dizocilpine (MK-801) was included in all solutions, at 1 μ M, to block NMDA receptor channels. **C**, Concentration-response relations for L-glutamate alone (\circ) (10 cells) or in the presence of 8 μ M 8-Me-DDHB (Δ) (six cells), 20 μ M 8-Me-DDHB (\blacksquare) (six cells), or 50 μ M 8-Me-DDHB (\bullet) (eight cells). Points, mean \pm standard error of the normalized currents (I/I_{max}). Smooth curves, best fit of eq. 2 to all of the data points for all four antagonist concentrations (0, 8, 20, and 50 μ M), with agonist $EC_{50} = 17$ μ M (15–19 μ M, 95% confidence interval), slope factor = 1.64 (1.47–1.80), and antagonist $K_B = 9.6$ μ M (7.8–11.8 μ M). Individual fits of eq. 1 were not significantly better, at the 5% level, than the simultaneous fit achieved with eq. 2 ($F_{5,117} = 1.17$).

DDHB, and 7-Me-DDHB were synthesized from the appropriately substituted 2-methoxy-1,4-naphthoquinones, according to the method of Birchall and Rees (33). The 3-acetyl ester and the 3-methyl ether of DDHB were synthesized from DDHB, as previously described (33). 4-Br-DDHB was prepared by bromination of DDHB, as described (33).

Benzazepines were dissolved in the standard external solution by sonication at 40°. Lack of visible precipitate after centrifugation at 3000 rpm for 5 min was considered evidence for complete dissolution. The maximal solubility of 8-Me-DDHB was approximately 50 μ M, whereas that of the other benzazepines was slightly higher. The parent molecule, DDHB, has previously been described (33) to undergo an intramolecular rearrangement to kynurenic acid, in the presence of aqueous base. The concentration of kynurenic acid in all of the solutions used for electrophysiological experiments was measured as previously described (34) and was found to be $<0.1\%$, on a molar basis.

Cell culture and electrophysiology. Neurons from the visual cortex of P0-postnatal day 5 Long Evans rat pups were dissociated with papain (Worthington Biochemical Corp.), as previously described

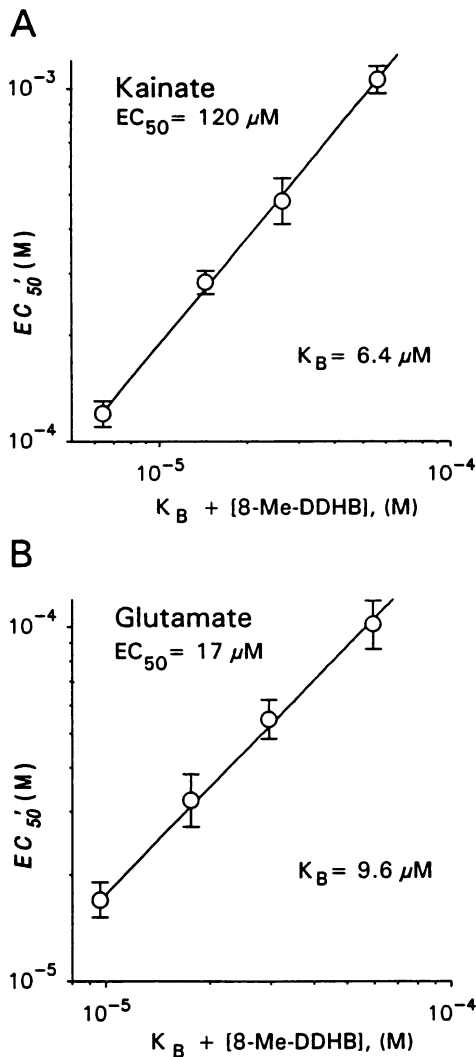


Fig. 6. 8-Me-DDHB produces simple competitive antagonism at non-NMDA receptors. *Points*, apparent half-maximal concentration of agonist ($EC_{50}' \pm 95\%$ confidence limits) determined from individual fits of eq. 1, plotted as a function of antagonist K_B plus antagonist concentration ($K_B + [8\text{-Me-DDHB}]$), for kainate (A) and L-glutamate (B). *Straight lines*, relationship expected for simple competitive antagonism given by the equation $EC_{50}' = (EC_{50}/K_B) \cdot (K_B + [\text{antagonist}])$. Values for EC_{50} and K_B were determined from the fit of eq. 2, as in Figs. 2 and 4. For kainate, $EC_{50} = 120 \mu\text{M}$; K_B for 8-Me-DDHB versus kainate = $6.4 \mu\text{M}$. For L-glutamate, $EC_{50} = 17 \mu\text{M}$; K_B for 8-Me-DDHB versus glutamate = $9.6 \mu\text{M}$.

(35). Cells were plated onto glial monolayers or directly onto glass coverslips coated with Cell-Tak (BioPolymers Inc.).

Tight-seal whole-cell recordings were obtained from cells that had been in culture for 6–14 days. Pipettes pulled from 100- μm Boralex micropipettes (Rochester Scientific Co., Inc.) were coated with Sylgard (Dow Corning Corp.) and fire polished. Pipette resistance ranged from 2 to 6 M Ω with 140 mM CsCH_3SO_3 , 5 mM CsCl , 10 mM EGTA, 10 mM HEPES, pH 7.4 (adjusted with CsOH), as the internal solution. The external solution for drug applications contained 160 mM NaCl , 2 mM CaCl_2 , 1 μM tetrodotoxin (Sigma), and 10 mM HEPES, pH 7.4. Dizocilpine (MK-801; donated by Merck, Sharp & Dohme) was added to the external solution at 1 μM for experiments with L-glutamate, to block current through channels gated by the NMDA receptor.

Drug solutions were applied by local perfusion from a linear array of eight microcapillary tubes (2- μm Drummond microcaps, 64-mm length). Solution flow was driven by gravity in most cases. For rapid applications of L-glutamate, the solutions were driven by a peristaltic pump and flow to the microcapillary tubes was gated by a set of three-

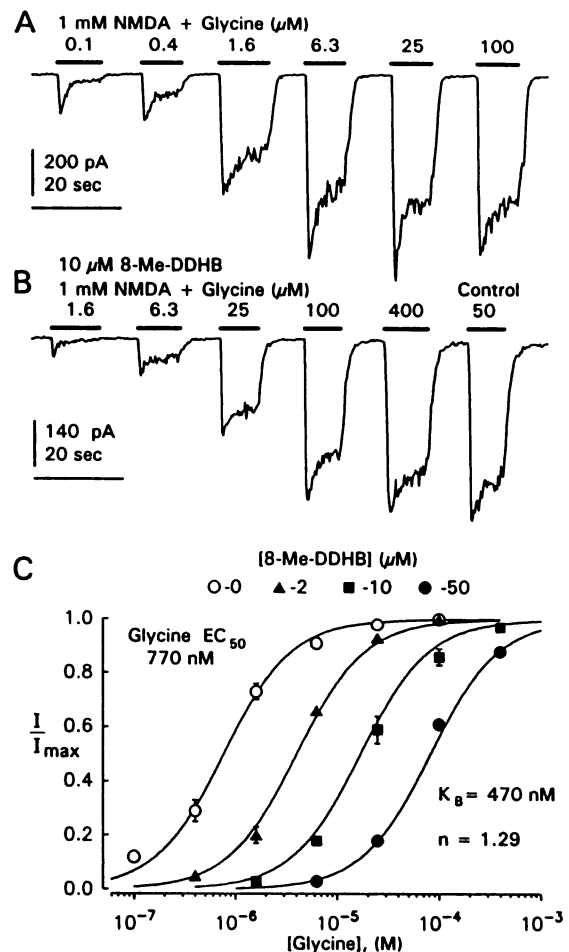


Fig. 7. Competitive antagonism of glycine potentiation at the NMDA receptor by 8-Me-DDHB. *A*, Whole-cell currents elicited by 1 mM NMDA and six concentrations of glycine. *B*, In a different cell, currents gated by NMDA and five concentrations of glycine in the presence of 10 μM 8-Me-DDHB, as well as a control response to NMDA plus 50 μM glycine without antagonist. Holding potential, -70 mV . *C*, Concentration-response relations for glycine alone (\circ) (15 applications in five cells) or in the presence of 2 μM 8-Me-DDHB (\blacktriangle) (eight applications in four cells), 10 μM 8-Me-DDHB (\blacksquare) (nine applications in three cells), or 50 μM 8-Me-DDHB (\bullet) (13 applications in four cells). *Points*, mean \pm standard error of the normalized currents (I/I_{max}). *Smooth curves*, best fit of eq. 2 to all of the data points for all four antagonist concentrations (0, 2, 10, and 50 μM), with agonist $EC_{50} = 770 \text{ nM}$ (690–850 nM, 95% confidence interval), slope factor = 1.29 (1.20–1.37), and antagonist $K_B = 470 \text{ nM}$ (410–540 nM). Individual fits of eq. 1 were not significantly better, at the 5% level, than the simultaneous fit achieved with eq. 2 ($F_{5,217} = 2.03$).

way valves (36). The bath was perfused at 1–5 ml/min with Tyrode's solution (150 mM NaCl , 4 mM KCl , 2 mM CaCl_2 , 2 mM MgCl_2 , 10 mM glucose, 10 mM HEPES, pH 7.4). Membrane potentials have been corrected for a junction potential of -10 mV between the internal solution and the Tyrode's solution in which seals were formed. Whole-cell currents recorded with a Dagan 3900 amplifier were filtered at 1 kHz (-3 dB , eight-pole Bessel) and digitized at 5 kHz. For storage and analysis, the data were compressed by averaging 3 msec of current at 0.1–0.5-sec intervals.

Experimental design and data analysis. Concentration-response curves were generated by applying a set of five to seven different agonist concentrations. In most experiments, each concentration was applied for 10–15 sec. Steady state currents were measured as the average current during the final third of each application. In most cells, the full set of applications was repeated several times. Because the absolute current levels varied from cell to cell, the values were normalized to the maximal current (I_{max}) produced by a saturating concentration of agonist. This control dose of agonist was included in every set

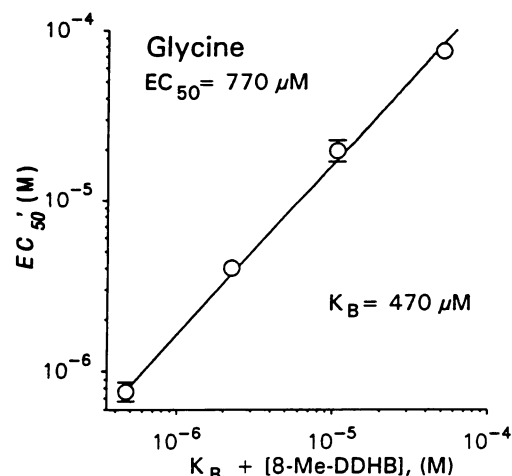


Fig. 8. 8-Me-DDHB produces simple competitive antagonism at the glycine allosteric site on the NMDA receptor. Points, apparent half-maximal concentration of agonist ($EC_{50}' \pm 95\%$ confidence limits) determined from individual fits of eq. 1, plotted as a function of antagonist K_B plus antagonist concentration ($K_B + [8\text{-Me-DDHB}]$). Straight line, relationship expected for simple competitive antagonism, given by the equation $EC_{50}' = (EC_{50}/K_B) \cdot (K_B + [\text{antagonist}])$. Values for EC_{50} and K_B were determined from the fit of eq. 2, as in Fig. 6. The EC_{50} for glycine = 770 nM; K_B for 8-Me-DDHB versus glycine = 470 nM.

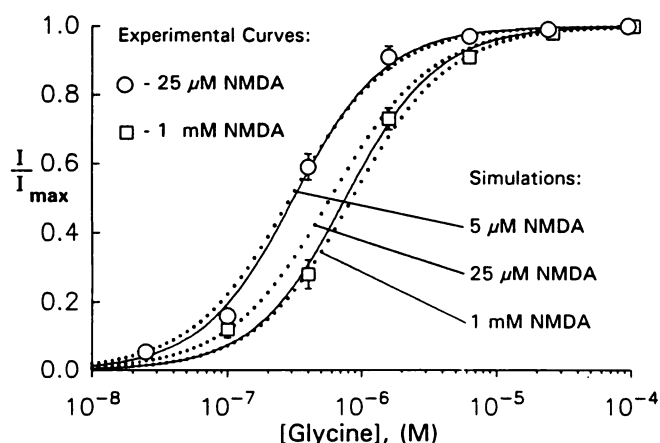


Fig. 9. Increasing concentrations of NMDA reduce the EC_{50} for glycine at the allosteric potentiation site. Concentration-response relations for glycine in the presence of 25 μM NMDA (O) (nine applications in four cells) or 1 mM NMDA (□) (15 applications in five cells). Points, mean \pm standard error of the normalized currents (I/I_{max}). Smooth curves, best fits of eq. 1 to all of the data points for each concentration of NMDA. With 25 μM NMDA, the EC_{50} for glycine was 308 nM (279–339 nM, 95% confidence interval; $n = 1.4$), compared with an EC_{50} of 770 nM (690–850 nM; $n = 1.3$) with 1 mM NMDA. Dotted lines, concentration-response relations for glycine predicted from computer simulations of scheme 2 of Benveniste et al. (49). The simulations yielded an EC_{50} for glycine of 294 nM ($n = 1.2$) when 5 μM NMDA was used, an EC_{50} of 586 nM ($n = 1.1$) for 25 μM NMDA, and an EC_{50} of 853 nM ($n = 1.2$) with 1 mM NMDA.

of applications. Currents evoked by a combination of agonist plus antagonist were normalized to the control (saturating) dose of agonist alone.

Nonlinear regression (Sigmaplot 4.1, Marquardt-Levenberg algorithm; Jandel Scientific) was used to fit the concentration-response data with the logistic equation (eq. 1):

$$\frac{I}{I_{\text{max}}} = \frac{1}{1 + \left(\frac{EC_{50}}{[\text{agonist}]} \right)^n} \quad (1)$$

where EC_{50} is the agonist concentration producing half-maximal activation and n is the slope factor. In several cases, the control dose-

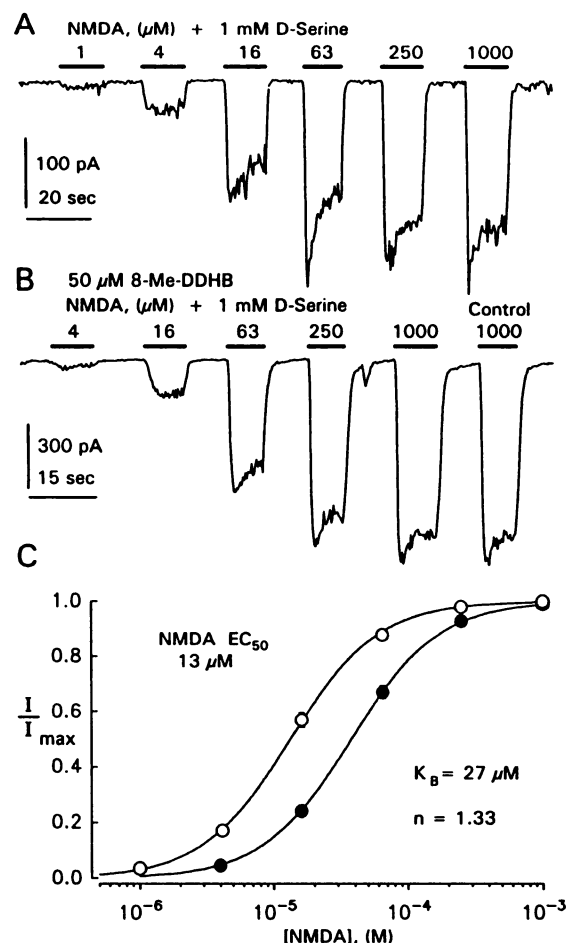


Fig. 10. Antagonism of the NMDA recognition site by 8-Me-DDHB. A, Currents elicited by 1 μM to 1 mM NMDA, all with 1 mM D-serine added to saturate the glycine allosteric site. B, In a different cell, currents gated by 4 μM to 1 mM NMDA in the presence of 50 μM 8-Me-DDHB and a control response to 1 mM NMDA without antagonist (all containing 1 mM D-serine). Holding potential, -70 mV. C, Concentration-response relations for NMDA plus 1 mM D-serine (O) (17 applications in seven cells) and in the presence of 50 μM 8-Me-DDHB (●) (nine applications in three cells). Points, mean \pm standard error of the normalized currents (I/I_{max}). Smooth curves, best fit of eq. 2 to all of the data points for 0 and 50 μM antagonist, with agonist $EC_{50} = 13$ μM (12–14 μM , 95% confidence interval), slope factor = 1.33 (1.25–1.42), and antagonist $K_B = 27$ μM (23–32 μM). Individual fits of eq. 1 were not significantly better, at the 5% level, than the simultaneous fit achieved with eq. 2 ($F_{1,136} = 0.58$).

response relation, for agonist alone, together with one to three agonist dose-response curves obtained in the presence of an antagonist were fit simultaneously, with the model for simple competitive antagonism (37–39) embodied in eq. 2 (40):

$$\frac{I}{I_{\text{max}}} = \frac{1}{1 + \left(\frac{(EC_{50}) \left(1 + \frac{[\text{antagonist}]}{K_B} \right)}{[\text{agonist}]} \right)^n} \quad (2)$$

where the parameters EC_{50} (the half-maximal dose of agonist alone), K_B (the antagonist dissociation constant), and n (the slope factor) were adjusted to provide an optimal fit of all of the curves at once. Eq. 2 constrains all of the concentration-response curves to be parallel and shifted from the control curve by the factor $(1 + [\text{antagonist}]/K_B)$. These constraints correspond to assuming a Schild slope of exactly -1 (39). The principal advantage of simultaneous fitting with eq. 2, in comparison with standard Schild analysis, is that the control concentration-response relation (agonist alone) is given equal weight, relative

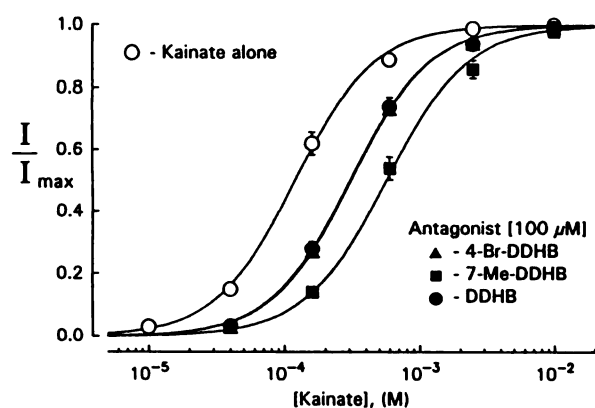


Fig. 11. Antagonism of kainate by DDHB, 4-Br-DDHB, and 7-Me-DDHB. Concentration-response relations for kainate alone (○) (15 applications in five cells) or in the presence of 100 μ M DDHB (●) (six applications in two cells), 100 μ M 4-Br-DDHB (△) (11 applications in two cells), or 100 μ M 7-Me-DDHB (■) (six applications in two cells). Points, mean \pm standard error of the normalized currents (I/I_{\max}). Smooth curves, best fits of eq. 1 to each concentration-response relation, with the slope factor constrained to be the same for all four curves. From the optimal fit, $n = 1.47$. Individual fitting of eq. 1 without the constraint of equivalent slopes was not significantly superior at the 5% level ($F_{3,185} = 0.63$). The K_B for each antagonist was determined from the best fit of eq. 2 to the antagonist and control data, with the slope factor held constant at the optimal value for all four curves ($n = 1.47$). For kainate alone, $EC_{50} = 120 \mu$ M (112–129 μ M, 95% confidence interval). With DDHB, the $EC_{50}' = 305 \mu$ M (279–333 μ M) and $K_B = 65 \mu$ M (53–80 μ M). With 4-Br-DDHB, the $EC_{50}' = 310 \mu$ M (288–335 μ M) and $K_B = 63 \mu$ M (53–74 μ M). With 7-Me-DDHB, the $EC_{50}' = 566 \mu$ M (511–627 μ M) and $K_B = 27 \mu$ M (22–32 μ M).

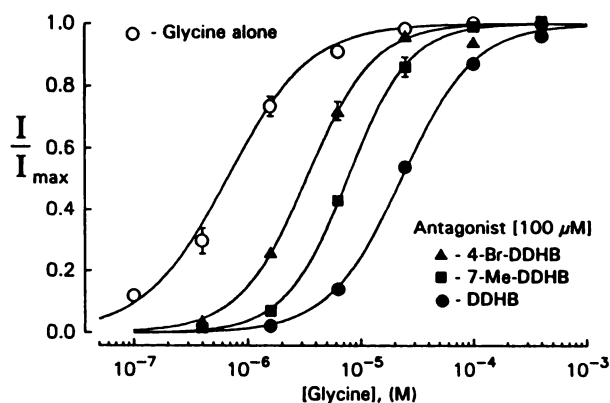


Fig. 12. Antagonism at the glycine allosteric site on NMDA receptors by 7-Me-DDHB, 4-Br-DDHB, and DDHB. All currents were activated by variable concentrations of glycine in the presence of 1 mM NMDA, to provide saturation of the NMDA recognition site. Concentration-response relations for glycine alone (○) (23 applications in eight cells) or in the presence of 100 μ M DDHB (●) (nine applications in two cells), 100 μ M 4-Br-DDHB (△) (10 applications in three cells), or 100 μ M 7-Me-DDHB (■) (10 applications in four cells). Points, mean \pm standard error of the normalized currents (I/I_{\max}). Smooth curves, best fits of eq. 1 to each concentration-response relation. For glycine alone, $EC_{50} = 665 \mu$ M (634–697 μ M, 95% confidence interval) and $n = 1.19$. With DDHB, the $EC_{50}' = 23 \mu$ M (22–24 μ M) and $n = 1.34$. With 4-Br-DDHB, the $EC_{50}' = 3.3 \mu$ M (3.2–3.5 μ M) and $n = 1.46$. With 7-Me-DDHB, the $EC_{50}' = 7.7 \mu$ M (7.4–8.4 μ M) and $n = 1.58$.

to the relations obtained in the presence of antagonist (40, 41). Furthermore, eq. 2 provides greater certainty in the value of K_B , because it is obtained from a direct fit of the experimental data, rather than from regression of calculated dose ratios. Plots of concentration-response relations shown in the figures display I/I_{\max} as the mean \pm

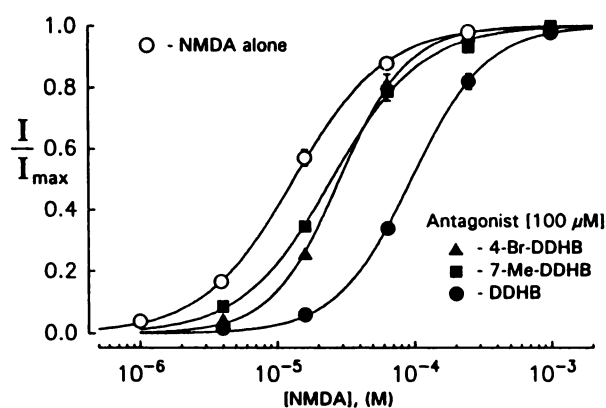


Fig. 13. Antagonism at the agonist recognition site on NMDA receptors by 7-Me-DDHB, 4-Br-DDHB, and DDHB. All currents were elicited by variable concentrations of NMDA in the presence of 1 mM D-serine, to saturate the glycine allosteric site. Concentration-response relations for NMDA alone (○) (17 applications in seven cells) or in the presence of 100 μ M DDHB (●) (11 applications in four cells), 100 μ M 4-Br-DDHB (△) (10 applications in three cells), or 100 μ M 7-Me-DDHB (■) (10 applications in three cells). Points, mean \pm standard error of the normalized currents (I/I_{\max}). Smooth curves, best fits of eq. 1 to each concentration-response relation. For NMDA alone, $EC_{50} = 13.2 \mu$ M (12.8–13.7 μ M, 95% confidence interval) and $n = 1.31$. With DDHB, the $EC_{50}' = 95 \mu$ M (92–99 μ M) and $n = 1.59$. With 4-Br-DDHB, the $EC_{50}' = 29 \mu$ M (28–30 μ M) and $n = 1.75$. With 7-Me-DDHB, the $EC_{50}' = 25 \mu$ M (24–26 μ M) and $n = 1.33$.

standard error for each agonist concentration. To ensure proper weighting, however, eqs. 1 and 2 were fit to all of the individual data points.

To test for statistically significant departure from the simple competitive model, the ratio of residual variance was calculated according to eq. 3 (40–42):

$$F_{df_1-df_2, df_1} = \frac{\left(\frac{SS_2 - SS_1}{df_1 - df_2} \right)}{\left(\frac{SS_1}{df_1} \right)} \quad (3)$$

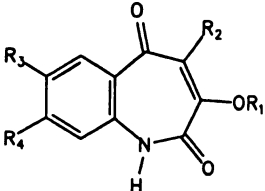
where SS_2 is the sum of squared deviations for the simultaneous fit with eq. 2, SS_1 is the total sum of squared deviations obtained when eq. 1 was fit to each concentration-response curve individually, and df_1 and df_2 are the degrees of freedom (number of data points – number of parameters) for individual fits with eq. 1 and the simultaneous fit with eq. 2, respectively. F values are given in the text in the form $F(df_1-df_2, df_1)$. Because EC_{50} and K_B are expected to exhibit log-normal distributions (42), the confidence intervals were obtained using the following substitutions in eqs. 1 and 2: $EC_{50} = 10^{-pE}$, where $pE = -\log EC_{50}$, and $K_B = 10^{-pK_B}$, where $pK_B = -\log K_B$. The 95% confidence intervals for pE and pK_B were calculated as the product of the standard deviation for each parameter (given by the fitting program) times the appropriate value from the t distribution. Confidence limits, as given in the text, have been transformed to EC_{50} and K_B .

Results

Benzazepines were tested as possible glutamate receptor antagonists because of their structural similarity to kynurenic acid and quinoxaline-2,3-dione. In preliminary experiments, DDHB was found to produce voltage-independent blockade of currents activated by half-maximal concentrations of L-glutamate, (+)-quisqualate, kainate, and NMDA. Fig. 2 shows the inhibition of kainate- and NMDA-gated currents by DDHB at holding potentials of +50 mV and –80 mV. At 100 μ M, DDHB blocked 40–45% of the current evoked by 100 μ M kainate and produced complete block of current activated by 20 μ M NMDA plus 300 nM glycine. Both the onset of and recovery from block

TABLE 1

Structure-activity relations for substituted benzazepines



Compound	R ₁	R ₂	R ₃	R ₄	Antagonist K _B ^a versus		
					Glycine	NMDA	Kainate
DDHB	H	H	H	H	3.0	16	65
8-Me-DDHB	H	H	H	CH ₃	0.47	27	6.4
7-Me-DDHB	H	H	CH ₃	H	9.5	108	27
4-Br-DDHB	H	Br	H	H	25	81	63
3-Methoxy-DDB	CH ₃	H	H	H	Inactive at 50 μM ^b		
3-Acetyl-DDB	CHOCH ₃	H	H	H	Inactive at 50 μM ^b		

^a Data for glycine come from Figs. 7 and 12, for NMDA from Figs. 10 and 13, and for kainate from Figs. 3 and 11.^b The two derivatives of DDB were tested at 50 μM against 100 μM kainate and against 20 μM NMDA plus 300 nM glycine; no inhibition was observed.

were complete within seconds. An initial screen of available derivatives of DDHB revealed that 8-Me-DDHB was the most potent antagonist and 4-Br-DDHB and 7-Me-DDHB were also active, whereas the 3-acetyl ester and the 3-methyl ether of DDB produced little or no inhibition of currents gated by any of the agonists. 8-Me-DDHB was selected for detailed analysis.

Antagonism at non-NMDA receptors by 8-Me-DDHB. Non-NMDA or kainate/AMPA receptor-linked channels can be activated by L-glutamate, quisqualate, kainate, and AMPA (1, 2). In order to evaluate quantitatively the affinity of 8-Me-DDHB for non-NMDA receptors, we determined the concentration-response relation for kainate and L-glutamate in the presence of 0, 8, 20, and 50 μM antagonist. As shown in Fig. 3, 8-Me-DDHB produced a concentration-dependent blockade of the current elicited by kainate. The inhibition produced by 8-Me-DDHB was completely overcome by increasing the concentration of kainate, a property expected for a competitive mechanism of antagonism. Following the method of Waud (40), the model for simple competitive antagonism embodied in eq. 2 was fit simultaneously to all four concentration-response curves shown in Fig. 3C. Eq. 2 uses the logistic curve (eq. 1) to describe the shape of the concentration-response relationship. This method incorporates the essential features of simple competitive antagonism (38, 39), because the addition of antagonist results in a parallel displacement of the control curve, obtained with agonist alone, by the factor $(1 + [\text{antagonist}]/K_B)$, where K_B is the antagonist dissociation constant.

As shown in Fig. 3C, the smooth curves defined by eq. 2 provide a good fit to the experimental data (see below; Fig. 6). The ratio of residual variance indicates that departure from the simple competitive model is not statistically significant at the 5% level ($F_{5, 197} = 0.71$). In agreement with previous work (13, 43, 44), kainate alone produced half-maximal activation at a concentration of 120 μM (111–131 μM, 95% confidence interval for EC₅₀ from the fit of eq. 2). 8-Me-DDHB antagonized the current gated by kainate with a K_B of 6.4 μM (5.5–7.5 μM).

Activation of non-NMDA receptors by L-glutamate was also inhibited by 8-Me-DDHB. L-Glutamate elicits both a transient and a sustained current when applied rapidly enough to central

neurons (onset, <30–50 msec) (11). As shown in Fig. 4, increasing concentrations of 8-Me-DDHB progressively blocked the fast transient current evoked by rapid application of 500 μM L-glutamate. (For all of the experiments with glutamate, 1 μM MK-801 was added to the external solutions, to suppress completely current through NMDA receptor channels.) The potency of 8-Me-DDHB as a non-NMDA receptor antagonist was evaluated quantitatively only for blockade of the sustained current. Antagonist affinity was not determined for the transient component of current because the null method used in eq. 2 requires that agonist and antagonist binding be at equilibrium (45). This is not likely to be the case at the peak of the transient current evoked by L-glutamate. Fig. 5C illustrates pooled steady state concentration-response data for the application of L-glutamate alone and in the presence of 8, 20, and 50 μM 8-Me-DDHB. In contrast to experiments with kainate, glycine, and NMDA, we observed considerable cell to cell variation in the EC₅₀ values obtained for application of L-glutamate, both in the absence and in the presence of 8-Me-DDHB. For this reason, a larger number of cells were tested with L-glutamate than was necessary with the other agonists. Although the source of this variability is not clear, it could potentially be due to differences in the extent of desensitization from one cell to another. In order to compensate for the fact that a different number of applications were performed on each cell, we first calculated the average normalized currents evoked by each concentration of agonist, on a cell by cell basis. Then, the mean and standard deviation of these individual cellular averages were computed for each agonist concentration over all cells tested. Using this approach, Fig. 5C shows that the control EC₅₀ for L-glutamate alone was 17 μM (15–19 μM, 95% confidence interval) and the K_B for 8-Me-DDHB, determined from the best fit of eq. 2, was 9.6 μM (7.8–11.8 μM). This control EC₅₀ for activation of steady state current by L-glutamate is consistent with that previously reported by others (43, 44, 46).

The two plots shown in Fig. 6 disclose the extent to which the concentration-response relations for kainate and L-glutamate diverge from the equation for competitive antagonism. The points show the control agonist EC₅₀ along with the agonist

concentration required to produce half-maximal activation (EC_{50}') in the presence of each antagonist concentration, obtained from the individual fits of the logistic equation (eq. 1). These values are plotted against the sum ($K_B + [\text{antagonist}]$), using the K_B given by the simultaneous fit of eq. 2. The straight lines in Fig. 6 represent the competitive relationship defined by $EC_{50}' = (EC_{50}/K_B) \cdot (K_B + [\text{antagonist}])$. For both kainate and L-glutamate, the points are well described by the theory. This form of display is similar to the Clark plot developed by Stone and Angus (41) (see also Ref. 47). In summary, these results are consistent with the action of 8-Me-DDHB as a simple competitive antagonist at the agonist recognition site on non-NMDA receptors, holding true when the channel is activated by either kainate ($K_B = 6.4 \mu\text{M}$) or L-glutamate ($K_B = 9.6 \mu\text{M}$).

Antagonism at the glycine allosteric site by 8-Me-DDHB. In preliminary experiments, benzazepines were found to inhibit currents elicited by submaximal concentrations of NMDA and glycine. Further work revealed that antagonism occurred both at the glycine allosteric site and at the transmitter binding site recognized by NMDA (see below). In order to study antagonism of the glycine site selectively, concentration-response relations for glycine were determined using a saturating level of NMDA (1 mM; see Fig. 10). A few of the cells in our cultures expressed strychnine-sensitive glycine receptors that activated a chloride-selective current; however, cells that displayed this current with high concentrations of glycine were excluded from the analysis. As shown in Fig. 6, 8-Me-DDHB at 2, 10, and 50 μM displaced the glycine dose-response relation toward progressively higher concentrations. The magnitudes of the shifts indicate a K_B of 470 nM (410–540 nM) for 8-Me-DDHB at the glycine site. The action of the drug is fully consistent with a mechanism of simple competitive antagonism, as shown by the parallel displacement of the glycine dose-response relations in Fig. 7 ($F_{5,217} = 2.03$; not significant at 5%) and by the plot in Fig. 8.

In the absence of antagonist, glycine potentiated the response to NMDA, with an EC_{50} of 770 nM (690–850 nM). This value is somewhat higher than previously reported EC_{50} values, which range from 90 to 700 nM (8, 10, 24, 30, 36, 48). Mayer and colleagues (36, 49) have recently proposed a model for desensitization of NMDA receptors in which binding of NMDA to the transmitter recognition site reduces the affinity for glycine at the allosteric potentiation site. Therefore, we considered whether the anomalously low affinity for glycine obtained in Fig. 7 could be due to the high concentration of NMDA (1 mM) used in this experiment. As shown in Fig. 9, the EC_{50} for potentiation of steady state current by glycine was sensitive to the concentration of NMDA. Glycine potentiated the current evoked by 25 μM NMDA with an EC_{50} of 310 nM, compared with an EC_{50} of nearly 800 nM when 1 mM NMDA was used. These results, which were obtained from sister cultures after 7 days *in vitro*, are in fairly close agreement with the model of Mayer and colleagues. The dotted lines shown in Fig. 9 represent the concentration-response relations for glycine with 5 μM , 25 μM , and 1 mM NMDA predicted by scheme 2 of Benveniste *et al.* (49). In the presence of 1 mM NMDA, the glycine EC_{50} of 853 nM predicted by their model falls just outside the 95% confidence interval of our experimental EC_{50} (690–850 nM). Consistent with previous reports (10, 30, 36, 48, 49), we obtained a significantly higher affinity for glycine potentiation of current gated by 25 μM NMDA. However, our experimental

EC_{50} for glycine of 308 nM (279–339 nM) was closer to the EC_{50} predicted by the model of Benveniste *et al.* (49) for 5 μM NMDA (294 nM) than to the value of 586 nM expected for 25 μM NMDA. The deviation of our results from their model may be due to the fact that our external solution contained 2 mM calcium, compared with 0.2 mM in the experiments modeled by Benveniste *et al.* (49). Calcium is known to influence the rate and extent of NMDA receptor desensitization (5, 36). There might also be differences as a result of age (Embryonic day 16–18 versus Postnatal day 0–5), species (mouse versus rat), or cell type (hippocampus versus cortex). It is interesting that the microscopic reversibility of the model of Benveniste *et al.* (49) requires that binding of glycine cause a reduction in the affinity for NMDA; however, such a reduction has not been observed, to our knowledge (8, 10).

Antagonism at the NMDA recognition site by 8-Me-DDHB. In addition to its action at the glycine allosteric site, 8-Me-DDHB also inhibits activation of the receptor by NMDA. As shown in Fig. 10, antagonist potency at the NMDA recognition site is approximately 60-fold lower than at the glycine allosteric site. Inhibition produced by 50 μM 8-Me-DDHB was completely overcome by increasing the concentration of NMDA. On the assumption that the interaction is competitive, the shift in the EC_{50} for NMDA from 13 to 28 μM after the addition of 50 μM 8-Me-DDHB indicates a K_B of 27 μM (23–32 μM). The control EC_{50} for NMDA (13 μM) is consistent with previous findings (10, 29, 43, 44). D-Serine (1 mM) (8, 9) was used in place of glycine for the experiments shown in Fig. 10, to avoid activation of chloride channels by strychnine-sensitive glycine receptors. Our preliminary experiments with 1 mM glycine revealed a similar shift in the EC_{50} for NMDA in cells that lacked the strychnine-sensitive glycine receptor. The fact that the inhibition produced by 50 μM 8-Me-DDHB was completely overcome by high concentrations of NMDA indicates that there was no appreciable binding of 8-Me-DDHB to the glycine allosteric site in the presence of 1 mM D-serine.

Structural analogues of 8-Me-DDHB. DDHB, 4-Br-DDHB, and 7-Me-DDHB were each tested, at a concentration of 100 μM , against kainate, glycine, and NMDA. As shown in Fig. 11, the three compounds shifted the kainate dose-response relation toward higher concentrations. 7-Me-DDHB produced the largest displacement, indicating a K_B of 27 μM (22–32 μM), compared with 63 μM (53–74 μM) for 4-Br-DDHB and 65 μM (53–80 μM) for DDHB. All three compounds were less potent than 8-Me-DDHB, which showed a K_B of 6.4 μM against kainate (Figs. 3 and 6). The four smooth curves fit to the data in Fig. 11 were constrained to be parallel, in accordance with the model for simple competitive antagonism. This constraint did not significantly reduce the goodness of fit, as determined by the ratio of residual variance ($F_{3,185} = 0.63$).

Fig. 12 shows the antagonism produced by 100 μM DDHB, 4-Br-DDHB, and 7-Me-DDHB at the glycine allosteric site on the NMDA receptor. All three compounds reduced the apparent affinity for glycine, and in each case the inhibition was overcome by adding a sufficiently high concentration of glycine (400 μM). To be fully consistent with the simple competitive mechanism of inhibition, the four concentration-response relations in Fig. 12 should be parallel. However, slight differences in the slopes of the four curves produced a significant departure from parallelism. The ratio of residual variance for comparing the fit obtained with parallel curves and individual fits of each dose-response relation with the logistic equation (eq. 1) was

$F_{3,271} = 4.64$ (significant at the 1% level). The four smooth curves shown in Fig. 12 represent individual fits of eq. 1 to the control data and to the data points for each of the three antagonists. The parameters for each curve are given in the legend to Fig. 12. Although the curves are not parallel, we calculated K_B values for the three antagonists assuming a competitive mechanism, in order to compare their potencies with that of 8-Me-DDHB. From the shift in the EC_{50} for glycine, the K_B for DDHB is estimated at $3.0 \mu\text{M}$, compared with $9.5 \mu\text{M}$ for 7-Me-DDHB and $25 \mu\text{M}$ for 4-Br-DDHB. These values are all significantly higher than the K_B of 470 nM obtained for 8-Me-DDHB (Fig. 7).

At the NMDA recognition site, antagonism by DDHB was found to be slightly more potent than that produced by 8-Me-DDHB. Fig. 13 shows the shifts produced by $100 \mu\text{M}$ DDHB, 4-Br-DDHB, and 7-Me-DDHB in the concentration-response relation for NMDA. All four curves were generated in the presence of 1 mM D-serine, to saturate the glycine potentiation site. NMDA at 1 mM completely overcame the inhibition produced by each of the three antagonists. The smooth curves shown in Fig. 13 are individual fits of eq. 1. When the four curves were constrained to have the same slope, the ratio of residual variance was significant at the 1% level ($F_{3,229} = 6.19$), which indicates that the data are not well described by four parallel curves. Nevertheless, K_B values were calculated for DDHB, 4-Br-DDHB, and 7-Me-DDHB using the assumption of competitive inhibition, in order to make a comparison with 8-Me-DDHB. The K_B calculated for DDHB from the data in Fig. 13 was $16 \mu\text{M}$, which is lower than the K_B value of $27 \mu\text{M}$ obtained for 8-Me-DDHB (Fig. 10). 7-Me-DDHB displayed a K_B of $108 \mu\text{M}$, whereas that for 4-Br-DDHB was $81 \mu\text{M}$.

Discussion

This study has shown that substituted benzazepines constitute a novel class of broad spectrum excitatory amino acid antagonists. Table 1 summarizes the structure-activity relationships for the four active derivatives, DDHB, 7-Me-DDHB, 8-Me-DDHB, and 4-Br-DDHB. All four compounds showed highest potency as antagonists of the glycine allosteric site on the NMDA receptor, with 8-Me-DDHB being the most potent derivative ($K_B = 470 \text{ nM}$ versus glycine). 8-Me-DDHB was approximately 14-fold less potent as an antagonist of non-NMDA receptors ($K_B = 6.4 \mu\text{M}$ versus kainate) and nearly 60-fold less effective at blocking the NMDA recognition site ($K_B = 27 \mu\text{M}$ versus NMDA). The parent compound, DDHB, demonstrated slightly higher affinity for the NMDA recognition site ($K_B = 16 \mu\text{M}$) than did the 8-methyl derivative, but DDHB was less potent than 8-Me-DDHB against glycine and kainate (DDHB $K_B = 3$ and $65 \mu\text{M}$, respectively).

Competitive antagonism. Two lines of evidence suggest that benzazepines inhibit the activation of excitatory amino acid receptors by a competitive mechanism of antagonism. First, the inhibition produced by all of the derivatives could be completely overcome by increasing the agonist concentration. Such a relief from blockade with saturating doses of agonist was observed for steady state activation of non-NMDA receptors by kainate or glutamate and for activation of NMDA receptors by both NMDA and glycine. Second, in the case of 8-Me-DDHB, which was tested at three different concentrations, the shifts produced in the concentration-response relations for kainate, glutamate, and glycine were well described by the simple competitive model of inhibition (37–39). For all

three agonists, the dose-response relations in the presence of 8-Me-DDHB were fit well by parallel curves shifted, relative to the control dose-response relation, by the factor $(1 + [8\text{-Me-DDHB}]/K_B)$. Separate fits of the logistic equation to each dose-response relation individually were not significantly better, at the 5% confidence level, than the simultaneous fit with parallel curves that conformed to the simple competitive relationship.

The logistic equation has been used widely to provide an empirical description of concentration-response relations (43, 44, 50). Although this equation does not correspond to any specific reaction scheme for channel activation (except for the special case of integral slope factor) (50), it has the advantages that the half-maximal point of the relationship is one of the fitted parameters and that the two parameters, EC_{50} and n , are not interdependent. When the logistic equation is used, slope factor values greater than 1 indicate that the receptor must bind more than one agonist molecule before the channel will open efficiently. In our experiments, the slope factors for the various agonists ranged from approximately 1.3 to 1.7. Similar results have been obtained in physiological experiments from several other laboratories (43, 44, 46). Although the simple competitive model of antagonism was developed with the assumption of a single agonist binding site, Colquhoun (51) and Thron (52) have shown that it also holds for many receptor mechanisms that involve binding of more than one agonist molecule. Colquhoun (45) has further elaborated the inhibition expected for a receptor with two nonequivalent sites, which may deviate from the simple competitive relationship in some cases.

A key feature of the simple competitive model is that a competitive inhibitor will exhibit the same K_B regardless of which agonist is used to activate the receptor; this property provides one of the main pharmacological tools for defining receptor subtypes (see Refs. 45 and 51). Our results for steady state antagonism of kainate and glutamate are in fairly good agreement with recent work (14, 15), which suggests that these two agonists activate the same population of receptors. 8-Me-DDHB inhibited kainate current with a K_B of $6.4 \mu\text{M}$ ($5.5\text{--}7.5 \mu\text{M}$, 95% confidence interval) and blocked steady state responses to glutamate with a K_B of $9.6 \mu\text{M}$ ($7.8\text{--}11.8 \mu\text{M}$, 95% confidence interval). Although the difference between these values reached statistical significance (Student's t test), the two K_B values are nearly the same. We consider the K_B against kainate to be the more reliable indicator of antagonist affinity for non-NMDA receptors, because of the greater variability that we observed in the concentration-response relations for glutamate (see Results). The reason for this variability is not clear. It could be due to the strong desensitization produced by glutamate or might possibly arise from heterogeneity in the expression of non-NMDA receptor subunits (14, 15). Further work is needed to explore these possibilities.

Structure-activity relations. The promise that glutamate receptor antagonists show as neuroprotective agents (19) has spurred an increasing effort to develop additional antagonists and to understand the structural determinants of antagonist affinity. With this aim, a large number of derivatives of the three parent compounds shown in Fig. 1, A–C, have recently been synthesized and tested for antagonist activity at the binding sites for glycine, NMDA, and kainate or AMPA (see Refs. 26 and 53–55). DDHB and its derivatives share a number of structural features with these parent compounds, kynurenic acid, indole-2-carboxylic acid, and quinoxaline-2,3-dione. Al-

though direct comparison of the potency of the four compounds in Fig. 1 is difficult, due to the different methods that have been used to assess antagonist affinity, the available data suggest that DDHB represents an attractive lead compound. DDHB acted at the glycine modulation site, the NMDA recognition site, and non-NMDA receptors, with apparent dissociation constants of 3, 16, and 65 μM , respectively (Table 1). For kynurenic acid (21–23, 26), inhibition constants of 15–41 μM have been measured against glycine, 154–325 μM against NMDA, and 82–132 μM against kainate, quisqualate, or AMPA. Unsubstituted quinoxaline-2,3-dione displays the following potency (23, 26): 26–39 μM versus glycine, 52 μM versus NMDA, and 120 μM versus kainate, quisqualate, or AMPA. Indole-2-carboxylic acid binds to the glycine site with a K_B of approximately 25 μM (10), but it has very low affinity for the other two sites ($K_B > 0.5\text{--}1\text{ mM}$).² Taken together, these values indicate that the antagonist potency of DDHB is equal to or greater than that of the other three parent compounds shown in Fig. 1.

Our results with substituted derivatives of DDHB fit quite well with observations made by Leeson *et al.* (26) on the potency of kynurenic acid derivatives. They found that methylation at the 7-position of kynurenic acid (which corresponds to the 8-position of DDHB) significantly improved the affinity for the glycine modulatory site. In contrast, addition of a 6-methyl group to kynurenic acid (corresponding to 7-Me-DDHB) reduced the antagonist potency against glycine but increased the affinity for non-NMDA receptors (26). Table 1 shows that 8-Me-DDHB was roughly 6-fold more potent against glycine than was DDHB, whereas 7-Me-DDHB was less potent than the parent compound at both the glycine and NMDA recognition sites but roughly twice as potent as DDHB against currents activated by kainate.

Halogen substitution of the benzene ring significantly enhances the affinity of kynurenic acid (22, 25, 26, 30), indole-2-carboxylic acid (10, 55), and quinoxaline-2,3-dione (30) both for the glycine modulatory site and for non-NMDA receptors. We found that 4-Br-DDHB, which is substituted on the heterocyclic ring, was unchanged, relative to DDHB, in its potency against kainate but was somewhat reduced in potency against both glycine and NMDA. It is tempting to speculate that a compound such as 6,8-dichloro-DDHB might be particularly potent as a glycine site antagonist, by analogy to 5,7-dichloro-kynurenic acid (25, 26) and 4,6-dichloroindole-2-carboxylic acid (55). Leeson *et al.* (26) have emphasized the importance of hydrophobic interactions in the enhancement of potency by substituents of the benzene ring, but electronegativity of the substituent groups may also play a role in determining antagonist affinity. Both energy calculations (54) and spectroscopic data (26, 56, 57) support the proposal (58) that the 4-keto tautomer of kynurenic acid, shown in Fig. 1A, predominates in aqueous solutions and may be the most likely form to interact with the receptor sites. Donation of a hydrogen bond by the 1-NH group (26) appears to be essential for receptor binding by all of the antagonists.

The lack of antagonism by the 3-acetyl ester and the 3-methyl ether of DDB (Table 1) suggests that the 3-hydroxyl group of DDHB is required for receptor binding. It seems likely that in DDHB, as well as the quinoxaline-2,3-diones, the oxygens at positions 2 and 3 exhibit partial anionic character (26,

58) and can, therefore, substitute for the carboxylate group of kynurenic acid, indole-2-carboxylic acid, and the various amino acid agonists. Finally, the oxygen at position 5 of DDHB may accept a hydrogen bond when binding to the glycine modulation site, as has been proposed for the 4-keto group of kynurenic acid (26), for various C-3 derivatives of indole-2-carboxylic acid (53), and for several small agonist compounds (48).

Bioavailability. Excessive activation of glutamate receptors causes damage to neurons and eventually leads to cell death (18). These neurotoxic actions of L-glutamate, and possibly other endogenous excitatory amino acids, have been implicated in a number of pathological conditions, including ischemia, epilepsy, and Huntington's disease (18, 19). Work on animal model systems suggests that glutamate receptor antagonists can protect neurons from the harmful effects of hyperstimulation; such neuroprotection has been observed with selective antagonists of both NMDA and non-NMDA receptors (19, 31). In order to be therapeutically useful, however, antagonists must gain access to the CNS, usually by entry from the periphery through the blood-brain barrier. Most competitive antagonists possess ionized groups at physiological pH and, therefore, penetrate the blood-brain barrier very poorly. In contrast, DDHB and its derivatives are uncharged and highly lipophilic at neutral pH, which suggests that they may enter the brain much more readily than many antagonists.

In the case of NMDA receptors, the necessity for passage into the CNS has focused attention on hydrophobic noncompetitive antagonists, such as phencyclidine and dizocilpine, which act by blocking the ion channel that is gated by NMDA. Although these compounds are neuroprotective, they also exhibit adverse side effects (59), including reinforcement of self-administration and possible direct toxic actions (60). Recent studies (reviewed in Ref. 59) suggest that competitive NMDA antagonists exhibit a different behavioral profile with fewer of the undesirable psychotomimetic effects that are characteristic of phencyclidine and related compounds.

As mentioned above, recent work (19, 31) indicates that both NMDA and non-NMDA receptor antagonists may contribute separately to neuroprotection. Of the four unsubstituted parent compounds shown in Fig. 1, DDHB has the highest apparent affinity at the glycine allosteric site, at the NMDA recognition site, and at non-NMDA receptors. Although antagonists with dual action at NMDA (glycine) and non-NMDA receptors are likely to cause more depression of neuronal function, they may prove especially valuable in countering the heterogeneity of pathological mechanisms that occur during ischemia. Our preliminary experiments indicate that DDHB is neuroprotective in both *in vitro* and *in vivo* assays.³ Further work is warranted to assess the potential therapeutic value of substituted benzazepines.

Acknowledgments

We are grateful to Bruce Bean for his support and encouragement.

³ K. J. Swartz and W. J., Koroshetz, unpublished observations.

References

1. Mayer, M. L., and G. L. Westbrook. The physiology of excitatory amino acids in the vertebrate central nervous system. *Prog. Neurobiol.* 28:197–276 (1987).
2. Dingledine, R., L. M. Boland, N. L. Chamberlin, K. Kawasaki, N. W. Kleckner, S. F. Traynelis, and T. A. Verdoorn. Amino acid receptors and uptake systems in the mammalian central nervous system. *Crit. Rev. Neurobiol.* 4:1–96 (1988).

² J. E. Huettner, unpublished observations.

3. Ascher, P., and L. Nowak. The role of divalent cations in the *N*-methyl-D-aspartate responses of mouse central neurones in culture. *J. Physiol. (Lond.)* **399**:247-266 (1988).
4. Mayer, M. L., and G. L. Westbrook. Permeation and block of *N*-methyl-D-aspartic acid receptor channels by divalent cations in mouse cultured central neurones. *J. Physiol. (Lond.)* **394**:501-527 (1987).
5. Mayer, M. L., and G. L. Westbrook. The action of *N*-methyl-D-aspartic acid on mouse spinal neurones in culture. *J. Physiol. (Lond.)* **361**:65-90 (1985).
6. Nowak, L., P. Bregestovski, P. Ascher, A. Herbet, and A. Prochiantz. Magnesium gates glutamate-activated channels in mouse central neurones. *Nature (Lond.)* **307**:462-465 (1984).
7. Johnson, J. W., and P. Ascher. Glycine potentiates the NMDA response in cultured mouse brain neurones. *Nature (Lond.)* **325**:529-531 (1987).
8. Kleckner, N. W., and R. Dingledine. Requirement for glycine in activation of NMDA-receptors expressed in *Xenopus* oocytes. *Science (Washington D. C.)* **241**:835-837 (1988).
9. Snell, L. D., R. S. Morter, and K. M. Johnson. Structural requirements for activation of the glycine receptor that modulates the *N*-methyl-D-aspartate operated ion channel. *Eur. J. Pharmacol.* **156**:105-110 (1988).
10. Huettner, J. E. Indole-2-carboxylic acid: a competitive antagonist of potentiation by glycine at the NMDA receptor. *Science (Washington D. C.)* **243**:1611-1613 (1989).
11. Kiskin, N. I., O. A. Krishtal, and A. Y. Tsyndrenko. Excitatory amino acid receptors in hippocampal neurones: kainate fails to desensitize them. *Neurosci. Lett.* **63**:225-230 (1986).
12. Iino, M., S. Ozawa, and K. Tsuzuki. Permeation of calcium through excitatory amino acid receptor channels in cultured rat hippocampal neurones. *J. Physiol. (Lond.)* **424**:151-165 (1990).
13. Huettner, J. Glutamate receptor channels in rat DRG neurones: activation by kainate and quisqualate and blockade of desensitization by Con A. *Neuron* **5**:255-266 (1990).
14. Boulter, J., M. Hollmann, A. O'Shea-Greenfield, M. Hartley, E. Deneris, C. Maron, and S. Heinemann. Molecular cloning and functional expression of glutamate receptor subunit genes. *Science (Washington D. C.)* **249**:1033-1037 (1990).
15. Keinänen, K., W. Wisden, B. Sommer, P. Werner, A. Herb, T. A. Verdoorn, B. Sakmann, and P. H. Seeburg. A family of AMPA-selective glutamate receptors. *Science (Washington D. C.)* **249**:556-560 (1990).
16. Miller, R. J. Metabotropic excitatory amino acid receptors reveal their true colors. *Trends Pharmacol. Sci.* **12**:365-367 (1991).
17. Collingridge, G. L., and W. Singer. Excitatory amino acid receptors and synaptic plasticity. *Trends Pharmacol. Sci.* **11**:290-296 (1990).
18. Choi, D. W. Glutamate neurotoxicity and diseases of the nervous system. *Neuron* **1**:623-634 (1988).
19. Meldrum, B., and J. Garthwaite. Excitatory amino acid neurotoxicity and neurodegenerative disease. *Trends Pharmacol. Sci.* **11**:379-387 (1990).
20. Perkins, M. N., and T. W. Stone. An ionophoretic investigation of the actions of convulsant kynurenes and their interactions with the endogenous excitant quinolinic acid. *Brain Res.* **247**:184-187 (1982).
21. Birch, P. J., C. J. Grossman, and A. G. Hayes. Kynurenate antagonizes responses to NMDA via an action at the strychnine-insensitive glycine receptor. *Eur. J. Pharmacol.* **154**:85-87 (1988).
22. Kemp, J. A., A. C. Foster, P. D. Leeson, T. Priestley, R. Tridgett, L. L. Iversen, and G. N. Woodruff. 7-Chlorokynurenic acid is a selective antagonist at the glycine modulatory site of the *N*-methyl-D-aspartate receptor complex. *Proc. Natl. Acad. Sci. USA* **85**:6547-6550 (1988).
23. Kessler, M., T. Terramani, G. Lynch, and M. Baudry. A glycine site associated with *N*-methyl-D-aspartic acid receptors: characterization and identification of a new class of antagonists. *J. Neurochem.* **52**:1319-1328 (1989).
24. Henderson, G., J. W. Johnson, and P. Ascher. Competitive antagonists and partial agonists at the glycine modulatory site of the mouse *N*-methyl-D-aspartate receptor. *J. Physiol. (Lond.)* **430**:189-212 (1990).
25. Baron, B. M., B. L. Harrison, F. P. Miller, I. A. McDonald, G. Salituro, C. J. Schmidt, S. M. Sorensen, H. S. White, and M. G. Palfreyman. Activity of 5,7-dichlorokynurenic acid, a potent antagonist at the *N*-methyl-D-aspartate receptor-associated glycine binding site. *Mol. Pharmacol.* **38**:554-561 (1990).
26. Leeson, P. D., R. Baker, R. W. Carling, N. R. Curtis, K. W. Moore, B. J. Williams, A. C. Foster, A. E. Donald, J. A. Kemp, and G. R. Marshall. Kynurenic acid derivatives: structure-activity relationships for excitatory amino acid antagonism and identification of potent and selective antagonists at the glycine site on the *N*-methyl-D-aspartate receptor. *J. Med. Chem.* **34**:1243-1252 (1991).
27. Honore, T., S. N. Davies, J. Drejer, E. J. Fletcher, P. Jacobsen, D. Lodge, and F. E. Nielsen. Quinoxalinediones: potent competitive non-NMDA glutamate receptor antagonists. *Science (Washington D. C.)* **241**:701-703 (1988).
28. Birch, P. J., C. J. Grossman, and A. G. Hayes. 6,7-Dinitro-quinoxaline-2,3-dione and 6-nitro,7-cyano-quinoxaline-2,3-dione antagonize responses to NMDA in the rat spinal cord via an action at the strychnine-insensitive glycine receptor. *Eur. J. Pharmacol.* **156**:177-180 (1988).
29. Verdoorn, T. A., N. W. Kleckner, and R. Dingledine. *N*-Methyl-D-aspartate/glycine and quisqualate/kainate receptors expressed in *Xenopus* oocytes: antagonist pharmacology. *Mol. Pharmacol.* **35**:360-368 (1989).
30. Kleckner, N. W., and R. Dingledine. Selectivity of quinoxalines and kynurenes as antagonists of the glycine site on *N*-methyl-D-aspartate receptors. *Mol. Pharmacol.* **36**:430-436 (1989).
31. Sheardown, M. J., E. O. Nielsen, A. J. Hansen, P. Jacobsen, and T. Honoré. 2,3-Dihydroxy-6-nitro-7-sulfamoyl-benzo(f)quinoxaline: a neuroprotectant for cerebral ischemia. *Science (Washington D. C.)* **247**:571-574 (1990).
32. Rees, A. H., and K. Simon. Some derivatives of 1-benzazepine. *Can. J. Chem.* **47**:1227-1239 (1969).
33. Birchall, G. R., and A. H. Rees. Some derivatives of 1-benzazepine. II. *Can. J. Chem.* **52**:610-615 (1974).
34. Swartz, K. J., W. R. Matson, U. MacGarvey, E. A. Ryan, and M. F. Beal. Measurement of kynurenic acid in mammalian brain extracts and cerebrospinal fluid by high-performance liquid chromatography with fluorometric and coulometric electrode array detection. *Anal. Biochem.* **185**:363-376 (1990).
35. Huettner, J. E., and R. W. Baughman. Primary culture of identified neurones from the visual cortex of postnatal rats. *J. Neurosci.* **6**:3044-3060 (1986).
36. Vyklícký, L., Jr., M. Benveniste, and M. L. Mayer. Modulation of *N*-methyl-D-aspartic acid receptor desensitization by glycine in cultured mouse hippocampal neurones. *J. Physiol. (Lond.)* **428**:313-331 (1990).
37. Clark, A. J. The antagonism of acetyl choline by atropine. *J. Physiol. (Lond.)* **61**:547-556 (1926).
38. Gaddum, J. H. The action of adrenalin and ergotamine on the uterus of the rabbit. *J. Physiol. (Lond.)* **61**:141-150 (1926).
39. Arunlakshana, O., and H. O. Schild. Some quantitative uses of drug antagonists. *Br. J. Pharmacol.* **14**:48-58 (1959).
40. Waud, D. R. Analysis of dose-response curves. *Methods Pharmacol.* **3**:471-506 (1975).
41. Stone, M., and J. A. Angus. Developments of computer-based estimation of pA_2 values and associated analysis. *J. Pharmacol. Exp. Ther.* **207**:705-718 (1978).
42. De Lean, A., A. A. Hancock, and R. J. Lefkowitz. Validation and statistical analysis of a computer modeling method for quantitative analysis of radioligand binding data for mixtures of pharmacological receptor subtypes. *Mol. Pharmacol.* **21**:5-16 (1982).
43. Verdoorn, T. A., and R. Dingledine. Excitatory amino acid receptors expressed in *Xenopus* oocytes: agonist pharmacology. *Mol. Pharmacol.* **34**:298-307 (1988).
44. Patneau, D. K., and M. L. Mayer. Structure-activity relationships for amino acid transmitter candidates acting at *N*-methyl-D-aspartate and quisqualate receptors. *J. Neurosci.* **10**:2385-2399 (1990).
45. Colquhoun, D. On the principles of postsynaptic action of neuromuscular blocking agents. *Handb. Exp. Pharmacol.* **59**:59-113 (1986).
46. O'Dell, T. J., and B. N. Christensen. A voltage-clamp study of isolated stingray horizontal cell non-NMDA excitatory amino acid receptors. *J. Neurophysiol.* **61**:162-172 (1989).
47. Stone, M. The Clark plot: a semi-historical case study. *J. Pharm. Pharmacol.* **32**:81-86 (1980).
48. McBain, C. J., N. W. Kleckner, S. Wyrick, and R. Dingledine. Structural requirements for activation of the glycine coagonist site of *N*-methyl-D-aspartate receptors expressed in *Xenopus* oocytes. *Mol. Pharmacol.* **36**:556-565 (1989).
49. Benveniste, M., J. Clements, L. Vyklícký, Jr., and M. L. Mayer. A kinetic analysis of the modulation of *N*-methyl-D-aspartic acid receptors by glycine in cultured mouse hippocampal neurones. *J. Physiol. (Lond.)* **428**:333-357 (1990).
50. Werman, R. An electrophysiological approach to drug-receptor mechanisms. *Comp. Biochem. Physiol.* **30**:997-1017 (1969).
51. Colquhoun, D. The relation between classical and cooperative models for drug action, in *Drug Receptors* (H. P. Rang, ed.). Macmillan, London, 149-182 (1973).
52. Thron, C. D. On the analysis of pharmacological experiments in terms of an allosteric receptor model. *Mol. Pharmacol.* **9**:1-9 (1973).
53. Gray, N., M. S. Dappen, B. K. Cheng, A. A. Cordi, J. P. Biesterfeldt, W. F. Hood, and J. B. Monahan. Novel indole-2-carboxylates as ligands for the strychnine-insensitive *N*-methyl-D-aspartate-linked glycine receptor. *J. Med. Chem.* **34**:1283-1292 (1991).
54. Harrison, B. L., B. M. Baron, D. M. Cousino, and I. A. McDonald. 4-[(Carboxymethyl)oxyl]- and 4-[(carboxymethyl)amino]-5,7-dichloroquinoxaline-2-carboxylic acid: new antagonists of the strychnine-insensitive glycine binding site on the *N*-methyl-D-aspartate receptor complex. *J. Med. Chem.* **33**:3130-3132 (1990).
55. Salituro, F. G., B. L. Harrison, B. M. Baron, P. L. Nyce, K. T. Stewart, and I. A. McDonald. 3-(2-Carboxyindole-3-yl)propionic acid derivatives: antagonists of the strychnine-insensitive glycine receptor associated with the *N*-methyl-D-aspartate receptor complex. *J. Med. Chem.* **33**:2944-2946 (1990).
56. El-Ezaby, M. S., T. M. Salem, M. M. Osman, and M. A. Makhayoun. Spectral studies on some quinoline derivatives of tryptophan metabolites. *Indian J. Chem.* **11**:1142-1145 (1973).

57. Pileni, M. P., M. Giraud, and R. Santus. Kynurenic acid. I. Spectroscopic properties. *Photochem. Photobiol.* **30**:251-256 (1979).
58. Huettner, J. E. Competitive antagonism of glycine at the *N*-methyl-D-aspartate (NMDA) receptor. *Biochem. Pharmacol.* **41**:9-16 (1991).
59. Willetts, J., R. L. Balster, and J. D. Leander. The behavioral pharmacology of NMDA receptor antagonists. *Trends Pharmacol. Sci.* **11**:423-428 (1990).
60. Olney, J. W., J. Labruyere, and M. T. Price. Pathological changes induced in

cerebrocortical neurons by phencyclidine and related drugs. *Science (Washington D. C.)* **244**:1360-1362 (1989).

Send reprint requests to: James E. Huettner, Department of Cell Biology and Physiology, Washington University Medical School, 660 South Euclid Avenue, Box 8228, St. Louis, MO 63110.
